GCB Bioenergy

WILEY

Global Change Biology Bioenergy
BIOPRODUCTS FOR A SUSTAINABLE BIOECONOMY

RESEARCH ARTICLE OPEN ACCESS

Combining Eddy Covariance Towers, Field Measurements, and the MEMS 2 Ecosystem Model Improves Confidence in the Climate Impacts of Bioenergy With Carbon Capture and Storage

Grant Falvo[1,2] | Yao Zhang[3,4] | Michael Abraha[2,5] | Samantha Mosier[1,2] | Yahn-Jauh Su[2,5] | Cheyenne Lei[6] | Jiquan Chen[2,5] | M. Francesca Cotrufo[3,4] | G. Philip Robertson[1,2]

[1]Department of Plant, Soil and Microbial Sciences, Michigan State University, East Lansing, Michigan, USA | [2]Great Lakes Bioenergy Research Center, East Lansing, Michigan, USA | [3]Department of Soil and Crop Sciences, Colorado State University, Fort Collins, Colorado, USA | [4]Natural Resource Ecology Laboratory, Fort Collins, Colorado, USA | [5]Department of Geography, Environment and Spatial Sciences, Michigan State University, East Lansing, Michigan, USA | [6]School of Environment and Sustainability, University of Michigan, Ann Arbor, Michigan, USA

Correspondence: Grant Falvo (grant.falvo@nau.edu)

Received: 17 October 2024 | **Revised:** 10 January 2025 | **Accepted:** 13 January 2025

Funding: This research was support by the Great Lakes Bioenergy Research Center, U.S. Department of Energy, Office of Science, Biological and Environmental Research Program under Award Number DE-SC0018409, by the National Science Foundation Long-term Ecological Research Program (DEB 2224712) at the Kellogg Biological Station, and by Michigan State University AgBioResearch.

Keywords: BECCS | climate change | ecosystem model | greenhouse gas | land use change | radiative forcing

ABSTRACT

Carbon dioxide removal technologies such as bioenergy with carbon capture and storage (BECCS) are required if the effects of climate change are to be reversed over the next century. However, BECCS demands extensive land use change that may create positive or negative radiative forcing impacts upstream of the BECCS facility through changes to in situ greenhouse gas fluxes and land surface albedo. When quantifying these upstream climate impacts, even at a single site, different methods can give different estimates. Here we show how three common methods for estimating the net ecosystem carbon balance of bioenergy crops established on former grassland or former cropland can differ in their central estimates and uncertainty. We place these net ecosystem carbon balance forcings in the context of associated radiative forcings from changes to soil N_2O and CH_4 fluxes, land surface albedo, embedded fossil fuel use, and geologically stored carbon. Results from long term eddy covariance measurements, a soil and plant carbon inventory, and the MEMS 2 process-based ecosystem model all agree that establishing perennials such as switchgrass or mixed prairie on former cropland resulted in net negative radiative forcing (i.e., global cooling) of −26.5 to −39.6 fW m^{-2} over 100 years. Establishing these perennials on former grassland sites had similar climate mitigation impacts of −19.3 to −42.5 fW m^{-2}. However, the largest climate mitigation came from establishing corn for BECCS on former cropland or grassland, with radiative forcings from −38.4 to −50.5 fW m^{-2}, due to its higher plant productivity and therefore more geologically stored carbon. Our results highlight the strengths and limitations of each method for quantifying the field scale climate impacts of BECCS and show that utilizing multiple methods can increase confidence in the final radiative forcing estimates.

1 | Introduction

Bioenergy with carbon capture and storage (BECCS) is projected to be necessary, in combination with reductions in fossil fuel use and other greenhouse gas mitigation measures, for keeping the anthropogenic rise in global atmospheric temperature to below 2°C by 2100 (Hanssen et al. 2020). In particular, carbon dioxide (CO_2) removal will be necessary to reverse the effects of climate change that extend well beyond 2100, such as sea level rise, with BECCS being a potentially key method for doing so at scale (Clark et al. 2016; Pett-Ridge et al. 2023). BECCS extracts energy from plant biomass through combustion, with the resulting CO_2 captured and stored in subsurface geologic formations. Proposals that use BECCS as a climate mitigation strategy have extensive land use requirements to produce enough plant biomass for meaningful carbon sequestration (Azar, Johansson, and Mattsson 2013). Some scenarios project land use requirements of up to $10\times10^6\,km^2$ by the year 2100 (Roe et al. 2019), which would make plant biomass production for BECCS the third largest land use globally, followed by agriculture ($48\times10^6\,km^2$) and forestry ($19\times10^6\,km^2$; FAO 2020, 2024). These extensive land use requirements motivate the study of the associated impacts on terrestrial ecosystems.

The environmental impacts associated with BECCS biomass production sites could be similar to those caused by moderately/intensively managed agricultural lands (Heck et al. 2018). These could include the near total loss of local flora and fauna populations within the field boundaries (Hanssen et al. 2022), the acceleration of soil erosion to unsustainable rates (Vogel, Deumlich, and Kaupenjohann 2016), and the pollution of streams and aquatic ecosystems with sediment, excess nitrogen and phosphorus, and pesticides (Diaz-Chavez et al. 2011). Furthermore, the fragmentation of native wildlife, insect, and plant habitat can have negative consequences for the biodiversity of nearby unmanaged landscapes (Immerzeel et al. 2014). However, substituting intensive annual crops for perennial native grasses or mixed native prairie species has been shown to ameliorate each of these environmental impacts to some degree (Gelfand et al. 2013; Werling et al. 2014). BECCS biomass production sites could also have social consequences, such as the competition for agricultural and forestry lands, farm labor, land tenure, and the increased need for machinery, fuel, and other necessary agricultural resources (Fajardy et al. 2021). Here we narrow the focus of this study to the global warming/cooling impacts that come from the sites were biomass is produced for BECCS.

While the primary mechanism that BECCS uses to reduce global radiative forcing is the storage of new plant biomass carbon in geologic formations, there are further contributions to radiative forcing that derive from biomass production sites. These include changes to (1) standing plant and soil carbon stocks, (2) soil nitrous oxide (N_2O) fluxes, (3) soil methane (CH_4) fluxes and (4) land surface albedo. However, the direction and magnitude of these radiative forcing contributions are uncertain due to the lack of long-term land use change experiments measuring these phenomena in a bioenergy context. Closing this knowledge gap is critical for constraining uncertainty in projections of how to achieve reduced radiative forcing with BECCS.

A common method for estimating the net ecosystem carbon balance (NECB) of the land converted to BECCS production is using a process-based ecosystem model that simulates a particular land use change scenario, relative to a baseline scenario (e.g., Lark et al. 2022). This is an attractive method as long term site-level simulations can be run in seconds on a typical modern computer. However, process-based ecosystem models have several drawbacks that can impact the final NECB of BECCS sites (Butnar et al. 2020). These include the parameterization of bioenergy crops like switchgrass or miscanthus in the plant submodules, which have relatively greater uncertainty in their parameter values due to their novelty in the modeling community. Much work on parameterizing the plant-related parameters of process-based ecosystem models has focused on broad plant functional types or the most commonly planted agricultural crops and less so on dedicated bioenergy crops (Shepherd, Martin, and Hastings 2021). Furthermore, estimating the initial plant and soil carbon stocks as affected by the previous land use at the site and correctly modeling the fate of that carbon further challenges model veracity. Finally, as is true with all model simulations, validation at a representative site with repeated in situ measurements of NECB is rare, adding further to the uncertainty of modeled results (Augusiak, Van Den Brink, and Grimm 2014; Le Noë et al. 2023).

Eddy covariance flux measurements are a second commonly used technology for estimating the NECB of BECCS production (Harris et al. 2017). By continuously measuring the net ecosystem exchange of CO_2 (NEE) and adjusting for other carbon pools that enter and leave a site (e.g., biomass via harvest and dissolved organic carbon via leaching), eddy covariance measurements can provide a spatially and temporally integrated in situ estimate of a site's NECB. While the eddy covariance method is an attractive option for this application, it too has several drawbacks that color the interpretation and use of its data. For instance, it is common for 30%–50% of flux measurements to be missing data due to low turbulence conditions or sensor malfunctions (Moffat et al. 2007). The seven towers used in this study had an average gap percentage of 37% during the study period. The gap filling methods required to calculate the NECB can also introduce bias and uncertainties in the flux estimates (Mahabbati et al. 2021). Arriving at a site's long term NECB requires the cumulative addition of all net ecosystem exchange measurements, meaning that any deviation in the systematic bias from zero, even if small, can add up over time to bias final (cumulative) NECB estimates.

Plant and soil carbon inventories are a third common method for estimating a site's NECB that requires measuring standing carbon stocks before and after a BECCS land use change event. This method is attractive because it can provide robust, well-defined, and trustworthy measurements of carbon stocks at the sample level. However, this method has several drawbacks mainly stem from the sampling effort required to achieve site-level estimates with acceptable uncertainties (Kravchenko and Robertson 2011). The size of each plot or soil sample is usually small compared to the size of the field. The natural heterogeneity of the field's carbon stocks necessitates taking numerous labor-intensive samples. While the carbon content of any individual sample can be derived with high accuracy and low uncertainty, the heterogeneity among samples and the lack of sufficient numbers of samples often results in relatively high uncertainty in the final NECB of plant and soil carbon inventories.

Most site-based studies of the NECB of BECCS production use only one or two of these three methods (e.g., Abraha et al. 2019; Gelfand et al. 2020; McCalmont et al. 2017; Melnikova et al. 2023). We are not aware of any study that compares all three approaches in the same experimental setting. Usually the circumstances of the site, experimental design, study duration, available measurements, and investigator expertise dictate the methods used in any one study. We suspect that the conclusions of these studies may change if a different method was used, especially if the study had a short duration.

Here we use a long term BECCS land use change experiment to compare three methods for quantifying each site's NECB over 13 years, namely (1) the MEMS 2 process-based ecosystem model, (2) the eddy covariance method, and (3) in situ inventories of plant and soil carbon stock changes. Our objectives are to (1) estimate the NECB of three proposed bioenergy production systems with contrasting land use history, (2) quantify the uncertainty of each of the three estimation methods and (3) place these NECB estimates in context of other sources of radiative forcing measured at the site, in particular, soil-atmosphere fluxes of N_2O and CH_4, embedded fossil fuel emissions, geologically stored carbon, as well as land surface albedo. We hypothesize that the NECB will be highest at sites with low initial ecosystem carbon stocks that transition to high belowground productivity plant types. Furthermore, we postulate that the eddy covariance method will have the lowest uncertainty in detecting these changes due to its comparatively large volume of data collection. Finally, apart from the geologically stored carbon, we expect the NECB to largely determine the overall radiative forcing budget of each site.

2 | Methods

2.1 | Site Description

The study site is located in southwestern Michigan, USA and was established by Michigan State University as part of the Great Lakes Bioenergy Research Center (42.4°N, 85.4°W, elevation 281 m). The mean annual temperature of the site is 9.3°C, the mean annual precipitation is 1067 mm, and there are on average 90 days with at least partial snow cover per year (Thornton et al. 2022). Soils at the site are well drained fine-loamy, mixed, active, mesic Typic Hapludalfs and consist of loamy glacial outwash overlying sand (Luehmann et al. 2016). Specifically, the mean soil texture across the study sites over the 0–50 cm depth profile was 66% sand, 26% silt, and 8% clay, while the 50–100 cm depth profile's soil texture was 81% sand, 12% silt, and 8% clay. Prior to industrial settlement of the area circa 1850, the site existed in a matrix of mid to late succession temperate deciduous broadleaf forests (Paciorek et al. 2021). Following more than a century of row crop agriculture, in 1987 one set of sites was converted to a perennial grassland (*Bromus inermis*) through enrollment in the USDA's Conservation Reserve Program (CRP), while the other set of sites continued to be used for row crop agriculture.

In 2009 the BECCS experiment was established by terminating all vegetation with herbicides at each site, except for one of the grassland sites that was maintained as a reference. In the initial year, herbicide resistant soybeans (*Glycine max*) were planted to allow further termination of preexisting vegetation. In 2010, either corn (*Zea mays*; planted annually), switchgrass (*Panicum virgatum*) or restored prairie (hereafter "prairie", a mixture of 19 species; see Abraha et al. 2019) were established on both the former grassland and former cropland sites. The field sizes range from 9 to 14 ha and were managed throughout the study period without tillage. The corn was planted each spring using a seed drill when the soil temperature was at a sufficiently warm level, field conditions were conducive to heavy machinery traffic, and the risk of frost was sufficiently low. The corn was fertilized with nitrogen at a rate of 180 kg N ha^{-1} $year^{-1}$, switchgrass at 56 kg N ha^{-1} $year^{-1}$, and prairie at 0 kg N ha^{-1} $year^{-1}$. From 2010 to 2014, only grain was harvested from the corn sites and the residue was left onsite, while from 2015 to 2021 both grain and residue were harvested. For the switchgrass and prairie sites, biomass was harvested annually in the Fall or Winter from 2011 to 2021. Harvests occurred after each crop had fully senesced and when field conditions were conducive to heavy machinery traffic, which different by crop type and by year-to-year weather conditions.

2.2 | Eddy Covariance Measurements

Each of the seven sites has had an eddy covariance tower in continuous operation since 2009 (Abraha et al. 2015; 2019). Each tower had an LI-7500 open-path infrared gas analyzer (LI-COR Biosciences, Lincoln, NE) that measures CO_2 and H_2O concentrations and a CSAT3 sonic anemometer (Campbell Scientific Inc., Logan, UT) that measures wind speed and direction. The infrared gas analyzers were calibrated (i.e., zero and spanned) every four to 6 months, rotated between the seven sites periodically. The sonic anemometer was kept at 1.5–2 m above the canopy by raising and lowering the tower each spring and fall as the vegetation height changed.

Details on other sensors installed at the sites and the processing of the high frequency data are provided in the Supporting Information. For the half-hourly flux data friction velocity thresholding, gap filling, and uncertainty estimation were conducted with the Reddyproc package in R (Wutzler et al. 2018). For each 3-month period of each year, 100 bootstrapped samples of data were used to estimate the distribution of probable friction velocity thresholds. The median, 2.5%, and 97.5% friction velocity thresholds were used for estimating the central, lower, and upper NEE estimates, respectively.

For each of the three friction velocity thresholds, the marginal distribution sampling algorithm following Reichstein et al. (2005) was used for gap filling the NEE and latent heat flux data. Artificial gaps at each observation were created to facilitate uncertainty estimation. The standard deviation of the look up table values for real gaps were used as the uncertainty estimate for the gap filling procedure. The standard deviation of the look up table values for artificial gaps were used as the uncertainty estimate for the measurement procedure. The final uncertainty in the cumulative NEE was calculated by numerical simulation. For 1000 simulations, a new NEE value was sampled at each half-hour interval from a normal distribution with the mean and standard deviation derived from the real and artificial

gap filling procedure described above. The median, 2.5% and 97.5% quantiles of the cumulative NEE from the 1000 simulations were used as the central, lower, and upper estimates for the eddy covariance method, respectively. The NECB was then calculated following Equation (1).

$$NECB = NEE - C_{Harvest} - DOC \quad (1)$$

where NEE is the net ecosystem exchange of CO_2, $C_{Harvest}$ is the carbon removed from the site (described below), and DOC is the dissolved organic carbon leached below the 100 cm soil depth. DOC losses are not measured by eddy covariance towers. We utilized the DOC output from the process-based ecosystem model as described below.

2.3 | Plant Biomass Measurements

All plant biomass that was removed from the site by machine for bioenergy production was measured directly by weighing harvested biomass on trucks and adjusting for their moisture content, which was measured by drying a subsample in an oven at 60°C. These values are provided in Table S1. Plant biomass weights were converted to plant carbon and nitrogen weights by measuring their carbon and nitrogen concentrations through dry combustion with an elemental analyzer (Costech ECS 4010 CHNSO Analyzer, CA, USA).

To quantify annual net primary productivity, plant biomass measurements were made annually from 2009 to 2016 at 10 geolocated sampling stations within each field by clipping, drying, and weighing 1 m^2 of live aboveground biomass. These values are provided in Table S1, as is their comparison to the mechanically harvest biomass mentioned above (i.e., their harvest efficiency). The shape of the quadrat used for the corn fields was 1.52 by 0.66 m and was placed across the rows to ensure representative sampling. The shape of the quadrat used for the switchgrass and prairie fields was 2.0 by 0.5 m. Surface litter was also collected from these stations simultaneously and weighed separately. Peak biomass sampling was timed to occur after most aboveground net primary production had occurred but before most senescence and biomass decomposition had taken place, usually in late August. Plant biomass weights were converted to plant carbon and nitrogen weights by measuring their carbon and nitrogen concentrations as above.

Belowground net primary production measurements were made annually from 2009 to 2017 through the use of the in-growth core technique (Lei et al. 2021). Briefly, a 30 cm deep soil core measuring 7 cm in diameter was excavated and roots were removed in the field. A cylinder of 5 mm mesh was placed in the excavated hole and the soil was replaced. Core installation occurred annually before the growing season began and remained in place for 12 months. Roots that had grown into the mesh cylinder were considered to represent the annual belowground net primary productivity.

Separately, standing belowground biomass carbon stocks were measured directly in Winter 2022 by taking a 7 cm diameter soil core to a depth of 25 cm to capture > 75% of root biomass. Cores were taken at each of the 10 georeferenced sampling stations in each of the seven fields. Roots were carefully washed with water from the soil on top of a 0.25 mm sieve, dried at 60°C and weighed. Root biomass weights were converted to root carbon and nitrogen weights by measuring their carbon and nitrogen concentrations as above.

2.4 | Soil Measurements

Soil sampling at each field's 10 georeferenced sampling stations occurred in 2009 before land use conversion and in 2014 and 2021 after the growing season ended for a total of 210 cores. Intact cores were taken from the 0 to 100 cm depth with a 6 or 7.6 cm diameter hydraulic probe and split into four sections by depth: 0–10 cm, 10–25 cm, 25–50 cm, and 50–100 cm. Surface litter was removed prior to inserting the probe. Soils were sieved to 4 mm by hand and roots were discarded. The coarse fragment > 4 mm was weighed as was the < 4 mm soil fraction after drying in a 60°C oven to constant weight. These weights were used to calculate the total and gravel-free bulk densities using the volume of the section. Subsamples of the soil were pulverized to a fine powder and stored in a desiccator for dry combustion analysis of their carbon and nitrogen concentrations. Each sample's carbon and nitrogen concentrations were measured with three technical replicates in an elemental analyzer.

Subsamples of the pulverized soil were also measured for mid-infrared (1.3–25 μm) spectroscopy (Ramírez et al. 2022). Samples were measured with four technical replicates with a Digilab FTS 7000 spectrometer (Varian Inc., CA, USA). Absorbance was obtained using a KBr background and deuterated triglycine sulfate detector. Each spectrum was made of 64 co-added scans at 2 cm^{-1} resolution.

2.5 | Soil Physical Fraction Measurements

We separated the mineral-associated from the particulate organic matter carbon and nitrogen concentrations, referred to as MAOM and POM, respectively, by size separation after mechanical aggregate dispersion (Cotrufo et al. 2019). A 10 g subsample of bulk soil was suspended in 0.5% sodium hexametaphosphate and 5 mm glass beads, shaken for 18 h, and then separated over a 53 μm sieve into POM (> 53 μm) and MAOM (< 53 μm), and dried in a 60°C oven to constant weight. Each fraction was weighed and pulverized for carbon and nitrogen concentration analyses as described above. Because this is a labor-intensive procedure, only a subset of 403 soil samples were processed directly. The remaining 437 MAOM and POM carbon and nitrogen fractions (e.g., g POM carbon g bulk $soil^{-1}$) were predicted from the MIR spectra (Ramírez et al. 2022). A partial least squares regression statistical model was constructed with the MIR spectra as predictors and the MAOM and POM carbon and nitrogen fractions as response variables. A minimized number of principal components and cross validation was used to limit out of sample errors associated with over fitting these types of models.

2.6 | Soil Gas Flux Measurements

Soil N_2O and CH_4 exchange was measured bi-weekly to monthly at four spatial locations within each site during

the growing season from 2009 to 2016 with the static chamber technique for a total of 3010 fluxes (Abraha et al. 2018). Briefly, 28 cm diameter metal cylinders were inserted 5 cm into the soil and covered with a lid for 1.5 h, over which four headspace gas samples were extracted and analyzed for N_2O and CH_4 concentrations in the lab with a gas chromatograph (7890A Agilent Technologies Inc., CA, USA) equipped with a ^{63}Ni electron capture detector (350°C), a Poropak Q column (1.8 m, 80/100 mesh) at 80°C, and a carrier gas of argon/methane (90/10). Changes in headspace gas concentrations were scaled to areal fluxes with the ideal gas law and assumed to represent the daily flux. Specifically, the four-point linear regression of concentration vs. time was visually inspected for outlier points (e.g., from a leaky vial), which were then discarded. We recognize the diurnal variability that exists for N_2O and CH_4 fluxes and believe that our decision to expend our limited time and resources on sampling the larger spatial and seasonal variability benefited this study most.

Separately, heterotrophic respiration was measured with 10 cm diameter metal cylinders that were installed 5 cm deep in the soil from 2011 to 2014 and kept free from live plant biomass through trenching and herbicide applications. Measurements were made during the growing season throughout the day in a ~bi-weekly fashion. A recirculating pump passed headspace air through an LICOR LI-7815 infrared gas analyzer (LICOR, NE, USA) and the change in CO_2 concentrations were similarly scaled to areal fluxes with the ideal gas law and assumed to represent the daily flux.

2.7 | Land Surface Albedo

Land surface albedo was measured for each experimental unit from 2009 to 2023 with the Landsat 5, 7, 8, and 9 satellites as well as the Sentinel 2A and 2B satellites following Wang et al. (2017) as the downward facing shortwave radiometers at these seven sites were not always extended out into the field they are meant to represent, that is, the tower they were mounted on was situated in a grassed buffer in the center of each field. The satellite data were acquired from Google Earth Engine. Shortwave broadband albedo was calculated using the albedo: reflectance ratio technique (Shuai et al. 2011, 2014; Wang et al. 2017). Landsat and Sentinel surface reflectance data are provided without surface anisotropy corrections, which are necessary to estimate land surface albedo. The bidirectional reflectance distribution function was used for this correction, with the parameters taken from the MCD43A1 V6.1 Bidirectional Reflectance Distribution Function and Albedo Model Parameters data product. See the Supporting Information for details on the data processing. Between 554 and 721 albedo observations that passed all quality screening criteria were available for each land use, resulting in a total of 4520 albedo observations measured from 2009 to 2023.

2.8 | Process-Based Ecosystem Modeling

The Microbial Efficiency and Matrix Stabilization model version 2.14 (MEMS 2) was used to solve daily carbon, nitrogen, water, and temperature fluxes at the field scale (Zhang et al. 2021). This 1-dimensional process-based ecosystem model requires initial condition and forcing data including, soil texture, soil bulk density, field management events, plant specific attributes (e.g., specific leaf area), air temperature, incoming shortwave radiation, precipitation, windspeed and relative humidity.

Initial conditions and forcing data were taken from the above-described soil, plant, and meteorological data. Additionally, a model spin-up period of 100 years was used before the start of the study period, which was January 1, 2009 to December 31, 2021. Soil carbon and nitrogen stocks in the POM and MAOM fractions at the beginning of the spin up period were set equally across all sites to allow the model to manifest the different land use histories (i.e., grassland or cropland from 1987 to 2008), and reach steady state by the start of the study period (January 1, 2009). Custom software was written in the R programing language to facilitate automated calibration and uncertainty estimation. The R package 'BayesianTools' was used to perform Markov-Chain Monte Carlo (MCMC) simulations of different parameter combinations (Lu et al. 2017). Parameters in the plant submodule were identified as the major sources of uncertainty in the final NECB. The chosen parameters are listed in Table S5. Uniform prior distributions for selected parameters were constructed from the plausible parameter value ranges listed in Table S5.

A likelihood-based cost function was used to calculate the difference between each observation and their associated model prediction (function *dnorm* in R). The following observations were used in the calibration scheme: eddy covariance NEE and latent heat flux, soil heterotrophic respiration, harvested plant biomass, peak plant biomass, root productivity, satellite vegetation index, soil total, and POM and MAOM carbon and nitrogen stocks. Likelihoods for each observation variable were summed to represent a global likelihood for each parameter set (Cameron et al. 2022). 10,000 MCMC simulations were conducted in parallel for each site as diagnostic plots showed acceptable convergence at this point. Following this calibration procedure, uncertainty in the final NECB was estimated by drawing a random set of parameters from the latter half of the MCMC simulations. After drawing 100 such sets, the median, 2.5%, and 97.5% quantiles of the final NECB were utilized as the central, lower, and upper estimates, respectfully.

2.9 | Radiative Forcing Calculations

Radiative forcing of CO_2, N_2O, CH_4, and land surface albedo were calculated over a 100-year timeline assuming that the changes during the 13-year study period represent the new steady state fluxes. The radiative forcing of each gas was modeled with their net exchange rates, atmospheric lifetimes, and radiative efficiencies following Neubauer and Megonigal (2015) and their associated correction (Neubauer and Megonigal 2019). This facilitated use of common units of fW m^{-2} and thus the direct use of top of atmosphere shortwave radiation fluxes. The atmospheric lifetime of N_2O and CH_4 was modeled according to Equation (2)

$$C_{i+1} = F_i + C_i \times e^{\left(-\frac{1}{L}\right)} \quad (2)$$

where C_i is thse atmospheric concentration in the ith year, F_i is the annual flux in the ith year, and L is the atmospheric lifetime

of the gas. The atmospheric lifetime of CO_2 was modeled according to Equation (3).

$$C_{i+1} = \sum_{p=1}^{4} (f_p * F_i) + C_{i,p} \times e^{\left(-\frac{1}{L_p}\right)} \quad (3)$$

where C_i is the atmospheric concentration in the ith year, f_p is the fraction of emissions associated with each pool, F_i is the annual flux in the ith year, $C_{i,p}$ is the atmospheric concentration of the pth pool in the ith year and L_p is the atmospheric lifetime of CO_2 in the pth pool. Radiative forcings for each gas were calculated as the product of the atmospheric concentration and the radiative efficiency. Constants for atmospheric lifetimes and pool fractions for Equations (2 and 3) can be found in Neubauer and Megonigal (2015, 2019), as can the constants for the radiative efficiencies of each gas.

Dissolved organic carbon (DOC) can be an important component of the NECB but it is not measured by eddy covariance towers. Furthermore, for the purpose of radiative forcing calculations, the fate of this DOC can alter the climate impacts of terrestrial land use changes. While DOC leaching was not measured directly in this study, the MEMS 2 model provides an estimate used here. We assumed in the radiative forcing calculations that 74% of DOC is eventually decomposed to CO_2 with a half-life of 2.5 years (Catalán et al. 2016; Ward et al. 2017).

Geologic storage of CO_2 captured during bioenergy production was modeled here according to Equation (4).

$$CO_2^{BECCS} = C_{harvest} \times E_{BECCS} \quad (4)$$

where CO_2^{BECCS} is the carbon stored in geologic formations, $C_{harvest}$ is the carbon harvested for bioenergy from each site, which was measured directly as described above, and E_{BECCS} is the total efficiency of the BECCS process in terms of CO_2 emitted during the processing stages. We utilize a value of 80% for E_{BECCS} following the integrated assessment model used in Klein et al. (2014).

The CO_2 emissions originating from fossil fuels used in synthetic nitrogen fertilizer production and field management operations were included here following Brentrup et al. (2018) and Gelfand et al. (2020), respectively. Synthetic nitrogen fertilizer application rates and field management activity information (expressed in terms of liters of fuel used) were used to calculate the amount of CO_2 emitted each year.

Top of atmosphere shortwave radiation fluxes were calculated with the measured land surface albedo and downwelling shortwave radiation measurements described above using Equation (5).

$$SW_{out}^{toa} = SW_{in} \times a \times T_{SW} \quad (5)$$

where SW_{out}^{toa} is the outgoing shortwave radiation at the top of the atmosphere, a is the land surface albedo, and T_{SW} is the all-sky transmittance of shortwave radiation through the atmosphere, calculated here as the ratio of top of atmosphere to bottom of atmosphere incoming shortwave radiation. Top of atmosphere incoming radiation was provided by the ERA5 reanalysis product (Hersbach et al. 2023). The radiative forcing from changes in albedo was estimated as the difference in annual average SW_{TOA} relative to a reference field. For the former grassland sites the reference field is the grassland site maintained as a reference. For the former cropland sites, the reference field is the former cropland site converted to corn.

2.10 | Statistical Analysis

Each eddy covariance tower measures each field as a whole. Therefore, as is common with eddy covariance studies, this experiment does not have replicated fields. Statistical differences within a treatment over time were assumed to be present when the 95% confidence intervals did not overlap with zero. Similarly, statistical differences between methods and sites were assumed to be present when their 95% confidence intervals did not overlap.

For the chamber based soil N_2O and CH_4 fluxes a generalized additive model was fit to account for the time periods between flux measurements. Fluxes at each site were predicted by a cyclic cubic regression spline of month as a continuous variable (i.e., December wraps around to January; Wood 2017). The mean annual fluxes of each site and their uncertainty were then extracted from this seasonal fit and used in the subsequent radiative forcing analysis.

For the carbon inventory methods NECB calculation, the longitudinal changes in plant and soil carbon stocks were used. The changes in soil organic carbon stocks were estimated by fitting a linear mixed effect model following Equation (6).

$$SOC = site \times depth \times year + r(site:station) \quad (6)$$

where, SOC is the bulk soil organic carbon stock in Mg C ha^{-1}, site is a categorical variable representing each study site, depth is a categorical variable representing the four depth intervals, year is a continuous variable representing the year of each soil sample, and r(site: station) is the random intercept for each station at each site. The changes in the other three components of the carbon (C) inventory method's NECB, namely roots and surface litter, were estimated directly using the winter 2022 sampling data. We assumed that all former grassland sites had the same root and surface litter biomass in 2009 as measured in the reference grassland site in 2022. Similarly, we assumed that all former cropland sites had the same root and surface litter biomass in 2009 as measured in the cropland site converted to corn in 2022. The 95% confidence interval of the final NECB for the C inventory method was calculated by arithmetic error propagation according to Equation (7).

$$NECB_{ci} = \sqrt{\sum ci_i^2} \quad (7)$$

where, $NECB_{ci}$ is the 95% confidence interval of the NECB, ci_i^2 is the squared 95% confidence interval of each i component, (i.e., soil, root, and surface litter).

3 | Results

3.1 | Net Ecosystem Carbon Balance Estimates

Here we report the range of the central estimates of the three methods, followed by the range of their 95% confidence intervals. Fully disaggregated results for each method and site

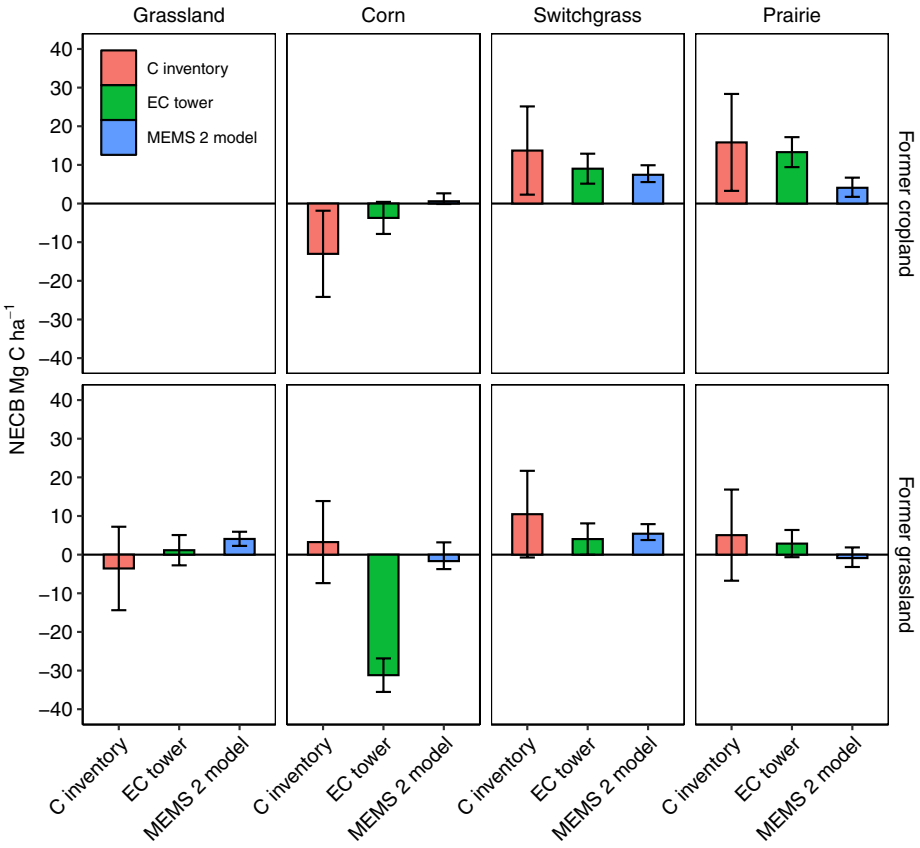

FIGURE 1 | The net ecosystem carbon balance (NECB) of each site and each method. Columns and error bars represent the central estimate and 95% confidence intervals, respectively. Positive values indicate carbon gained by the ecosystem and negative values indicate carbon lost from the ecosystem.

are reported in Figure 1 and Table S2. Over 13 years, switchgrass planted on former cropland sequestered between 9.0 and 13.7 Mg C ha^{-1} (95% CI 2.3–25.1) in all plant and soil components to a depth of 100 cm. Similarly, prairie established on former cropland sequestered between 4.1 and 15.8 Mg C ha^{-1} (95% CI 1.7–28.4) during the study period. The conversion of grassland to these same perennials had more carbon neutral results. Switchgrass planted on former grassland had a NECB between 4.6 and 10.5 Mg C ha^{-1} (95% CI −0.7 to 21.7). Similarly, for prairie established on former grassland, the NECB was between −0.9 and 5.0 Mg C ha^{-1} (95% CI −6.8 to 16.8). Corn had more variable NECB results with the former cropland site having a NECB of −13.0 to 0.6 Mg C ha^{-1} (95% CI −24.2 to 2.6) and the corn at the former grassland site having a NECB of −31.2 to 3.3 Mg C ha^{-1} (95% CI −38.8 to 13.9). The reference grassland site that was unmanaged and not harvested had a NECB of −3.6 to 4.1 Mg C ha^{-1} (95% CI −14.4 to 7.2).

3.2 | Plant and Soil Carbon Dynamics

While the eddy covariance method does not allow for the disaggregation of the NECB into its plant and soil components, our C inventory and the MEMS 2 model results show that surface litter, roots, POM, and MAOM carbon stock changes contributed to NECB changes of up to 3.4, 5.2, 14.7, and 12.7 Mg C ha^{-1}, respectively (Figure 2; Table S3). For surface litter, we found that changes in standing carbon stocks from the beginning to the end of the study period estimated using the C inventory method ranged from −1.6 Mg C ha^{-1} in the prairie established on former grassland to 0.0 Mg C ha^{-1} in the prairie on former cropland (Table S3). The MEMS 2 model estimated greater surface litter carbon loss, with a range of −3.4 Mg C ha^{-1} in the corn on former grassland to −0.2 Mg C ha^{-1} in the grassland reference site (Table S3).

For roots, changes in standing carbon stocks from the beginning to the end of the study period estimated using the C inventory method ranged from −2.0 Mg C ha^{-1} in the corn established on former grassland to 5.2 Mg C ha^{-1} in the prairie on former cropland (Table S3). The MEMS 2 model estimated lower root carbon gains with a range of −0.5 Mg C ha^{-1} in the corn on former grassland to 2.3 Mg C ha^{-1} in switchgrass on former cropland (Table S3).

For POM, changes in standing carbon stocks over the 0–100 cm depth profile from the beginning to the end of the study period estimated using the C inventory method ranged from −3.6 Mg C ha^{-1} in the corn established on former cropland to 14.7 Mg C ha^{-1} in the switchgrass on former grassland (Table S3). The MEMS 2 model estimated lower POM carbon gains with a range of −1.3 Mg C ha^{-1} in the corn on former grassland to 5.7 Mg C ha^{-1} in switchgrass on former grassland (Table S3).

For MAOM, changes in standing carbon stocks over the 0–100 cm depth profile from the beginning to the end of the study period

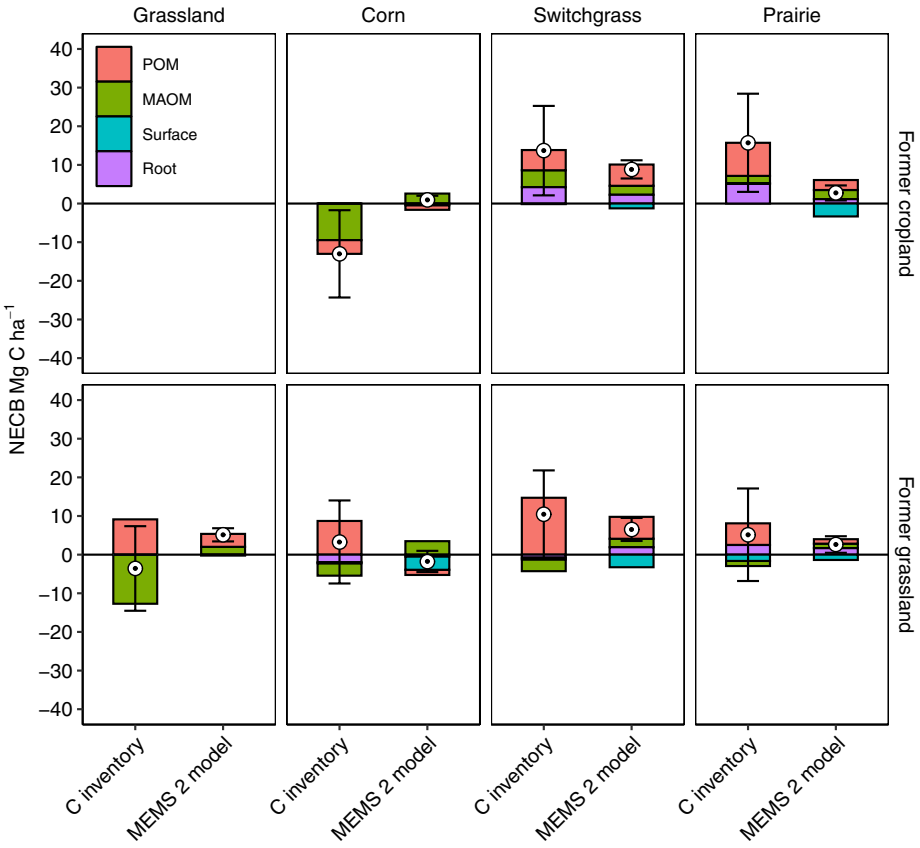

FIGURE 2 | The net ecosystem carbon balance (NECB) components of each site and each method. Columns represent each component. The points and error bars represent the net NECB central estimate and 95% confidence intervals, respectively. Positive values indicate carbon gained by the ecosystem and negative values indicate carbon lost from the ecosystem.

estimated using the C inventory method ranged from −12.7 Mg C ha^{-1} in the grassland reference site to 4.4 Mg C ha^{-1} in the switchgrass on former cropland (Table S3). The MEMS 2 model estimated greater MAOM carbon gains with a range of 1.2 Mg C ha^{-1} in the prairie on former grassland to 3.5 Mg C ha^{-1} in corn on former grassland (Table S3).

3.3 | Soil N_2O and CH_4

Soil gas fluxes derived from in situ measurements were affected by both the current and previous land use. Soil nitrous oxide emissions were highest in the sites fertilized with synthetic N. The corn site on former grassland had the highest emissions (0.67 g N_2O m^{-2} year^{-1}, s.e. 0.06, Figure S1), while the corn site on former cropland had lower emissions (0.44 g N_2O m^{-2} year^{-1}, s.e. 0.05). For the switchgrass grown on former grassland, N_2O emissions were lower at (0.17 g N_2O m^{-2} year^{-1}, s.e. 0.04), while the switchgrass grown on former cropland emitted N_2O at a similar rate (0.28 g N_2O m^{-2} year^{-1}, s.e. 0.05). Prairie on former grassland shared the lowest N_2O emissions (0.12 g N_2O m^{-2} year^{-1}, s.e. 0.04), along with prairie on former cropland (0.14 g N_2O m^{-2} year^{-1}, s.e. 0.04) and the grassland reference site (0.12 g N_2O m^{-2} year^{-1}, s.e. 0.04). Soil methane oxidation rates were highest at the prairie and switchgrass on former grassland sites (−0.14 and −0.11 g CH_4 m^{-2} year^{-1}, respectively, s.e. < 0.03). The other sites all had similarly low methane oxidation rates ranging from −0.03 to −0.08 g CH_4 m^{-2} year^{-1} (s.e. < 0.03).

3.4 | Albedo

Land use change and land use history altered the albedo of the land surface changing the outgoing shortwave radiation at the top of the atmosphere (SW^{toa}_{out}). The conversion of grassland to bioenergy crops increased the land surface albedo while the conversion of cropland to bioenergy crops reduced it. SW^{toa}_{out} in the corn, switchgrass, and prairie grown on the former grassland changed by 2.3, 3.0, and 2.2 W m^{-2} (s.e. < 0.2), respectively, relative to the grassland reference site (Figure S2). On the other hand, SW^{toa}_{out} in the switchgrass and prairie grown on the former cropland changed by −1.9 and − 1.3 (s.e. < 0.2), respectively, relative to the corn on former cropland.

3.5 | Radiative Forcing

Each component of the overall radiative forcing budget of each land use had a substantial effect on the net outcome, apart from soil methane oxidation, which was relatively minor. The largest component of the radiative forcing budget was the geologically stored carbon harvested from each site for BECCS. This component followed patterns of aboveground plant productivity with the corn on former grassland and cropland having the largest forcing of −56.3 and −45.8 fW m^{-2}, respectively (Figure 3; Tables S1 and S4). Switchgrass grown on former grassland and cropland had the next largest forcing with −36.0 and −28.1 fW m^{-2}, respectively. The lowest forcing from geologic storage of

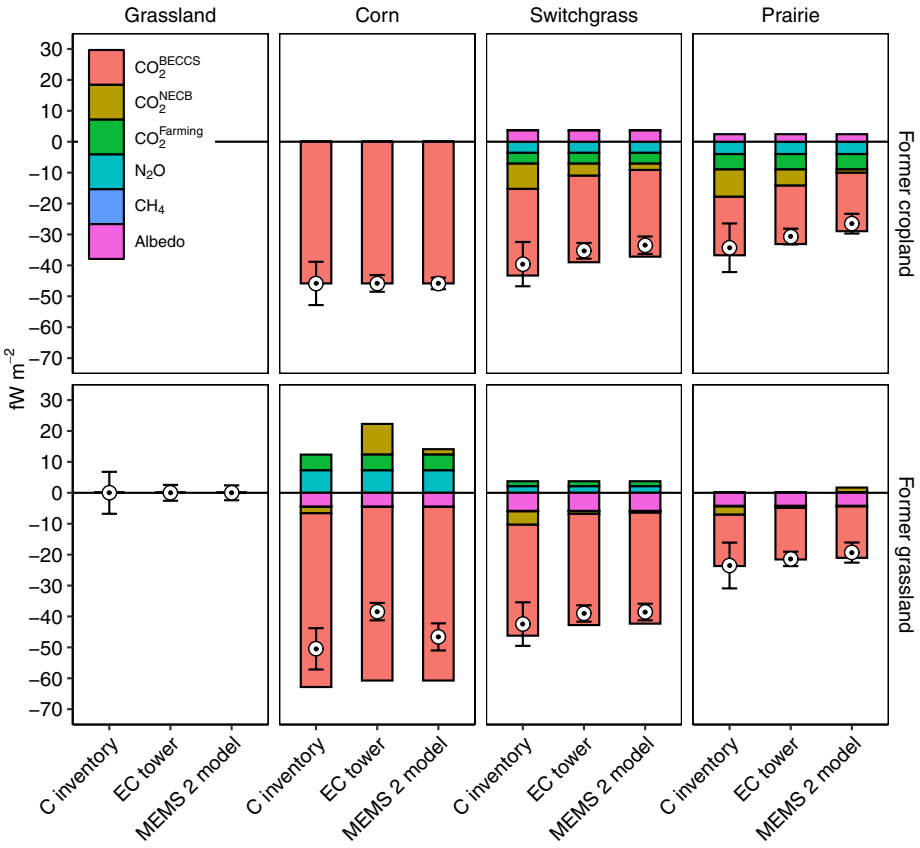

FIGURE 3 | Average instantaneous radiative forcing for each component and method during the 100-year period following the land use change event. The points and error bars represent the net radiative forcing central estimate and 95% confidence intervals, respectively. Positive values indicate a warming impact and negative values indicate a cooling impact, relative to their baseline scenario, which is set to zero by definition. Note that only the NECB differs by method.

harvested carbon came from the prairie on former grassland and cropland (−16.7 and −19.0 fW m^{-2}, respectively).

The radiative forcing from NECB CO_2, soil CH_4, soil N_2O, and albedo each follow the results reported above in their original flux units. However, the magnitude of each component's contribution to the overall radiative forcing budget follows a different scalar (Figure 3; Table S4). We summarize the net radiative forcing estimates here for each method and site, noting that the soil CH_4, soil N_2O, albedo, farming, and geologic CO_2 radiative forcings of each site are shared across each of the three methods (i.e., only the NECB radiative forcings of each site differ by method).

The corn on former grassland had the largest net negative radiative forcing with the C inventory, eddy covariance method, and MEMS 2 model methods yielding −50.5, −38.4, and −46.6 fW m^{-2}, respectively (Figure 3; Table S4). The corn on former cropland had the next largest net negative radiative forcing with each method yielding −45.8 fW m^{-2}. The switchgrass on former grassland had the next largest net negative radiative forcing with the C inventory, eddy covariance method, and MEMS 2 model methods yielding −42.5, −39.0, and −38.6 fW m^{-2}, respectively. The switchgrass on former cropland followed, with the C inventory, eddy covariance method, and MEMS 2 model methods yielding −39.6, −35.3, and −33.5 fW m^{-2}, respectively. The prairie on former cropland had the next lowest net negative radiative forcing with the C inventory, eddy covariance method, and MEMS 2 model methods yielding −34.3, −30.7, and −26.5 fW m^{-2}, respectively. Finally, the prairie on former grassland had the lowest net negative radiative forcing with the C inventory, eddy covariance method, and MEMS 2 model methods yielding −23.5, −21.4, and −19.3 fW m^{-2}, respectively. The reference grassland site, being a baseline reference, had a neutral radiative forcing by definition.

4 | Discussion

4.1 | Net Ecosystem Carbon Balance

Producing biomass for BECCS from corn, switchgrass, and prairie grown on former grassland and former cropland resulted in net climate change mitigation. However, the method for estimating NECB impacted the portion of climate mitigation attributed to in situ CO_2. Our NECB results show that the C inventory method had on average the highest uncertainty (22.7 Mg C ha^{-1} 95% CI), followed by the eddy covariance method (7.9 Mg C ha^{-1}) and then the MEMS 2 model (4.6 Mg C ha^{-1}; Table S2). The magnitude of NECB estimates tended to be largest with the C inventory in comparison to the eddy covariance method and the MEMS 2 model, which had somewhat more carbon neutral results.

However, one exception is the NECB for the corn grown on the former grassland site (US-KM1) where the eddy covariance tower suggested a change of −31.2 Mg C ha^{-1} (95% CI −35.5 to −26.9 Mg C ha^{-1}; Table S2) over the 13-year study period. This change corresponds to a 52% reduction of the site's total ecosystem carbon stocks (60.5 Mg C ha^{-1}), which is excessive and almost certainly in error. Moreover, the tower-based NECB does not agree with the C inventory or MEMS 2 model at the site, which suggest a small sink or a small source (3.3 and −1.7 Mg C ha^{-1}, respectively). After careful consideration and much scrutiny by our team and the outside experts we solicited, we have yet to find a satisfactory explanation for this disparity. We are inclined to believe that the direction of the suggested change (i.e., net loss) is consistent with a change from grassland to cropland. However, the robust results obtained by our repeated soil and plant carbon stock measurements, as well as the MEMS 2 model, give us the confidence to be able to conclude that this tower's estimate of such a large and rapid carbon loss is significantly biased. That is, the 95% confidence intervals of the NECB at this site from the other two methods are not close to overlapping with the EC tower's.

Changes in POM, MAOM, roots, and surface litter each contributed to the overall NECB. While they differed in magnitude, both the C inventory and the MEMS 2 model agree that, on average, NECB changes were attributed most to POM (7.9 and 3.0 Mg C ha^{-1}, respectively), then MAOM (5.2 and 2.3 Mg C ha^{-1}, respectively), followed by roots (2.1 and 1.1 Mg C ha^{-1}, respectively), and finally surface litter (0.4 and 1.9 Mg C ha^{-1}, respectively), though that order differed by site (Table S3). Roots were more of a contributor to carbon sequestration in the perennials as compared to the corn and reference grassland where soil C differences dominated.

If well designed and calibrated, process-based ecosystem models are an attractive option for estimating the NECB of BECCS landscapes as they are straightforward and inexpensive to set up and run quickly (although their development, calibration, and validation can be quite involved; Cheng et al. 2024, Muri 2018). On the other hand, in situ plant and soil sampling are labor intensive, expensive to carry out, and can require waiting years for ecological changes to take place (Chatterjee et al. 2009). Eddy covariance towers similarly require waiting for ecological changes to take place and are also expensive but, they can be relatively less labor intensive than plant and soil sampling (Baldocchi 2014). The ideal measurement technique will vary given the set of research sites, questions, and resources (Smith et al. 2020).

4.2 | Soil N_2O

Changes in soil N_2O emissions tracked differences in the synthetic nitrogen fertilization management regime. Converting highly fertilized cropland to lower or zero nitrogen fertilization rates in switchgrass and prairie, resulted in negative radiative forcing impacts of −3.5 and −4.0 fW m^{-2}, respectively. On the other hand, converting unfertilized grasslands to corn, switchgrass, and prairie (high, low, and zero nitrogen fertilization rates) corresponded to N_2O related radiative forcings of 7.3, 2.1, and 0.0 fW m^{-2}, respectively. Other studies of N_2O emissions following changes in land use have shown that nitrogen fertilization is a key determinant of emission strength and timing (McDaniel et al. 2019).

4.3 | Albedo

Changes to land surface albedo followed changes in both inherent canopy reflectance properties as well as the height of standing biomass during periods of snow cover. During periods without snow cover, switchgrass and prairie were relatively brighter than the reference grassland site but were relatively darker than the continuous corn on the former cropland. Planting corn on former grassland also yielded a more reflective land surface during periods without snow cover. When snow was present, the lower stature vegetation of harvested fields allowed for more unobstructed reflectance of shortwave radiation from the snow surface. These phenomena led us to conclude that establishing perennial bioenergy crops on former cropland resulted in positive radiative forcing due to albedo change (i.e., warming; 2.3–3.6 fW m^{-2}; Table S4) while establishing bioenergy crops on former grassland resulted in negative radiative forcing due to albedo change (i.e., cooling; −4.2 to −5.8 fW m^{-2}; Table S4). Other studies of land use change and land surface albedo have found that both the inherent reflectivity of the vegetation as well as the covering of snow in the high latitudes are important drivers of land surface albedo changes (Abraha et al. 2021; Cai et al. 2016; Lei, Chen, and Robertson 2023).

4.4 | Bioenergy With Carbon Capture and Storage

More productive lands can support greater storage of atmospheric carbon in geologic formations, the main climate benefit of BECCS (García-Freites, Gough, and Röder 2021; Rosa, Sanchez, and Mazzotti 2021). The corn provided more biomass for BECCS than switchgrass or prairie, resulting in more negative radiative forcing (i.e., cooling). Furthermore, the former grassland sites had higher productivity than the former cropland sites, except when planted to mixed prairie, where both sites were equally productive (Table S1). From the perspective of climate mitigation, the reference grassland is penalized because it is not harvested for BECCS. The potential onsite carbon sequestration of establishing an unmanaged grassland can be inferred here from the differences in initial ecosystem carbon stocks with the grassland and cropland sites. While this difference is substantial, the carbon storage potential is limited and saturates over time, creating an opportunity cost, that can grow indefinitely, of not cultivating crops and storing the carbon in geologic formations with BECCS. This suggests that, from a climate perspective, enrolling former cropland in conservation grassland programs could provide mitigation, but utilizing former cropland for BECCS can provide even more climate mitigation (Robertson et al. 2017; Stoy et al. 2018).

4.5 | Radiative Forcing

BECCS commands its popularity as an idea from the substantial carbon removal potential it can deliver and our study is no exception in showing these potentials (Fajardy and Mac Dowell 2017;

Fridahl and Lehtveer 2018). Each of the bioenergy crops we examined provided substantial climate mitigation whether they were grown on former cropland or former grassland. Switchgrass and prairie established on former cropland resulted in net negative radiative forcing −26.5 to −39.6 fW m^{-2}, while establishing the same perennials on former grassland resulted in a similar −19.3 to −42.5 fW m^{-2}. The two corn sites had the greatest climate mitigation potential of −45.8 to −50.5 fW m^{-2}.

Geologic storage of harvested biomass carbon was, on average, the largest component of the radiative forcing budget (33.6 fW m^{-2}), followed by on site NECB (1.1–4.4 fW m^{-2}), albedo (3.4 fW m^{-2}), N_2O (2.8 fW m^{-2}), farming-related fossil fuels (2.6 fW m^{-2}) and CH_4 (0.1 fW m^{-2}; Table S4). Previous work has shown the differences in energy return and climate impact for annual vs. perennial bioenergy crops can stem from the amount of resources required for maintaining the fields (e.g., diesel fuel for machinery; Bennett et al. 2021; Felten et al, 2013). We also found this to be a substantial contributor to the net climate impact of each scenario as the fossil fuels embedded in nitrogen fertilizer and farming activities considered here had climate impacts on roughly the same order as the NECB, N_2O emissions, and albedo. However, the main climate impact of BECCS (i.e., storing atmospheric carbon in geological formations) outweighed these differences as the crops with the largest change in fossil fuel use (e.g., corn planted on former grassland) were also the most productive, and the extra stored carbon compensated for this in terms of climate mitigation.

For former cropland, newly sequestered carbon by the perennials and reductions in soil N_2O emissions contributed to climate mitigation potentials. However, a less reflective land surface offset some of this mitigation (Figure 3). Due to the difference in previous land use, the albedo changes on the former grassland had the opposite effect (i.e., net negative radiative forcing). This finding suggests that the location of new BECCS sites and its current albedo are important considerations for climate mitigation (Baik et al. 2018).

4.6 | Broader Impacts

The gap between the amount of land needed to achieve meaningful climate mitigation with BECCS and the amount of land currently dedicated to it is nearly as large as it was when the idea was first proposed (Guo, Song, and Buhain 2015; Ma et al. 2022). The current amount of plant biomass carbon being stored in dedicated geologic formations is 0.32 Tg C $year^{-1}$ or 0.008% of the proposed 4000 Tg C $year^{-1}$ needed by some scenarios in 2100 (Daniels 2023; Roe et al. 2019). Resistance to adoption can be attributed to an array of complex social and ecological factors (Donnison et al. 2020).

A key aim of BECCS is to provide climate mitigation while minimizing impacts to nature and society (Quader and Ahmed 2017). Concerns about BECCS conflicting with food production have led to the focus on so-called 'marginal lands' (Smith et al. 2019). Our study found that intensively managing corn on productive lands provided the greatest climate mitigation potential due to its high productivity, demonstrating a tradeoff in maximizing climate mitigation and food production. That said, we found that less productive, former cropland planted to less productive perennials also provided substantial climate benefits and required less intensive management. Furthermore, utilizing less productive former cropland avoids the conversion of already established natural areas and preserves the biodiversity and ecosystem services that those lands currently provide (Grass et al. 2019). However, considerable stretches of grassland are planted to monocultures of introduced species, suggesting that replacing those monocultures with switchgrass or prairie and harvesting the biomass for BECCS could provide similar or greater biodiversity and ecosystem services while simultaneously increasing the climate mitigation that those lands can provide (Bardgett et al. 2021; Dixon et al. 2014; Gerstner et al. 2014). Although, this would come at a cost to food production, among other concerns. While the debate over how to best use land is ongoing, our study enriches the discussion by providing information to land managers and decision makers about how the climate impacts of BECCS can factor into the tradeoffs involved in balancing other social and environmental goals.

Author Contributions

Grant Falvo: conceptualization, data curation, formal analysis, methodology, software, visualization, writing – original draft, writing – review and editing. **Yao Zhang:** methodology, software, writing – review and editing. **Michael Abraha:** data curation, formal analysis, methodology, software, writing – review and editing. **Samantha Mosier:** data curation, methodology, writing – review and editing. **Yahn-Jauh Su:** data curation, methodology, writing – review and editing. **Cheyenne Lei:** data curation, methodology, writing – review and editing. **Jiquan Chen:** data curation, funding acquisition, project administration, supervision, writing – review and editing. **M. Francesca Cotrufo:** data curation, funding acquisition, project administration, supervision, writing – review and editing. **G. Philip Robertson:** data curation, funding acquisition, project administration, supervision, writing – review and editing.

Acknowledgements

We would like to thank Sven Bohm, Kevin Kahmark, Jane Schuette, Joseph Simmons, Katie Steeves, Stacey Vanderwulp, Brook Wilke, and Kaija Windeler for their help in collecting data, maintaining the fields, and improving this manuscript.

Conflicts of Interest

The authors declare no conflicts of interest.

Data Availability Statement

Data and code are available at Dryad https://doi.org/10.5061/dryad.qrfj6q5s5.

References

Abraha, M., J. Chen, H. Chu, et al. 2015. "Evapotranspiration of Annual and Perennial Biofuel Crops in a Variable Climate." *Global Change Biology. Bioenergy* 7, no. 6: 1344–1356. https://doi.org/10.1111/gcbb.12239.

Abraha, M., J. Chen, S. K. Hamilton, et al. 2021. "Albedo-Induced Global Warming Impact of Conservation Reserve Program Grasslands Converted to Annual and Perennial Bioenergy Crops." *Environmental Research Letters* 16, no. 8: 84059. https://doi.org/10.1088/1748-9326/ac1815.

Abraha, M., I. Gelfand, S. K. Hamilton, J. Chen, and G. P. Robertson. 2018. "Legacy Effects of Land Use on Soil Nitrous Oxide Emissions

in Annual Crop and Perennial Grassland Ecosystems." *Ecological Applications* 28, no. 5: 1362–1369. https://doi.org/10.1002/eap.1745.

Abraha, M., I. Gelfand, S. K. Hamilton, J. Chen, and G. P. Robertson. 2019. "Carbon Debt of Field-Scale Conservation Reserve Program Grasslands Converted to Annual and Perennial Bioenergy Crops." *Environmental Research Letters* 14, no. 2: 024019.

Augusiak, J., P. J. Van Den Brink, and V. Grimm. 2014. "Merging Validation and Evaluation of Ecological Models to 'Evaludation': A Review of Terminology and a Practical Approach." *Ecological Modelling* 280: 117–128. https://doi.org/10.1016/j.ecolmodel.2013.11.009.

Azar, C., D. J. A. Johansson, and N. Mattsson. 2013. "Meeting Global Temperature Targets—The Role of Bioenergy With Carbon Capture and Storage." *Environmental Research Letters* 8, no. 3: 034004. https://doi.org/10.1088/1748-9326/8/3/034004.

Baik, E., D. L. Sanchez, P. A. Turner, K. J. Mach, C. B. Field, and S. M. Benson. 2018. "Geospatial Analysis of Near-Term Potential for Carbon-Negative Bioenergy in the United States." *Proceedings of the National Academy of Sciences* 115, no. 13: 3290–3295. https://doi.org/10.1073/pnas.1720338115.

Baldocchi, D. 2014. "Measuring Fluxes of Trace Gases and Energy Between Ecosystems and the Atmosphere – The State and Future of the Eddy Covariance Method." *Global Change Biology* 20, no. 12: 3600–3609. https://doi.org/10.1111/gcb.12649.

Bardgett, R. D., J. M. Bullock, S. Lavorel, et al. 2021. "Combatting Global Grassland Degradation." *Nature Reviews Earth and Environment* 2, no. 10: 720–735. https://doi.org/10.1038/s43017-021-00207-2.

Bennett, J. A., M. Abotalib, F. Zhao, and A. F. Clarens. 2021. "Life Cycle Meta-Analysis of Carbon Capture Pathways in Power Plants: Implications for Bioenergy With Carbon Capture and Storage." *International Journal of Greenhouse Gas Control* 111: 103468. https://doi.org/10.1016/j.ijggc.2021.103468.

Brentrup, F., J. Lammel, T. Stephani, and B. Christensen. 2018. "Updated Carbon Footprint Values for Mineral Fertilizer From Different World Regions." International Conference on Green and Sustainable Innovation. October 17 2018.

Butnar, I., P. H. Li, N. Strachan, J. Portugal Pereira, A. Gambhir, and P. Smith. 2020. "A Deep Dive Into the Modelling Assumptions for Biomass With Carbon Capture and Storage (BECCS): A Transparency Exercise." *Environmental Research Letters* 15, no. 8: 084008.

Cai, H., J. Wang, Y. Feng, M. Wang, Z. Qin, and J. B. Dunn. 2016. "Consideration of Land Use Change-Induced Surface Albedo Effects in Life-Cycle Analysis of Biofuels." *Energy & Environmental Science* 9, no. 9: 2855–2867. https://doi.org/10.1039/C6EE01728B.

Cameron, D., F. Hartig, F. Minnuno, et al. 2022. "Issues in Calibrating Models With Multiple Unbalanced Constraints: The Significance of Systematic Model and Data Errors." *Methods in Ecology and Evolution* 13, no. 12: 2757–2770. https://doi.org/10.1111/2041-210X.14002.

Catalán, N., R. Marcé, D. N. Kothawala, and L. J. Tranvik. 2016. "Organic Carbon Decomposition Rates Controlled by Water Retention Time Across Inland Waters." *Nature Geoscience* 9, no. 7: 501–504. https://doi.org/10.1038/ngeo2720.

Chatterjee, A., R. Lal, L. Wielopolski, M. Z. Martin, and M. H. Ebinger. 2009. "Evaluation of Different Soil Carbon Determination Methods." *Critical Reviews in Plant Sciences* 28, no. 3: 164–178. https://doi.org/10.1080/07352680902776556.

Cheng, Y., D. M. Lawrence, M. Pan, et al. 2024. "A Bioenergy-Focused Versus a Reforestation-Focused Mitigation Pathway Yields Disparate Carbon Storage and Climate Responses." *Proceedings of the National Academy of Sciences* 121, no. 7: e2306775121. https://doi.org/10.1073/pnas.2306775121.

Clark, P. U., J. D. Shakun, S. A. Marcott, et al. 2016. "Consequences of Twenty-First-Century Policy for Multi-Millennial Climate and Sea-Level Change." *Nature Climate Change* 6, no. 4: 360–369. https://doi.org/10.1038/nclimate2923.

Cotrufo, M. F., M. G. Ranalli, M. L. Haddix, J. Six, and E. Lugato. 2019. "Soil Carbon Storage Informed by Particulate and Mineral-Associated Organic Matter." *Nature Geoscience* 12, no. 12: 989–994.

Daniels, J. 2023. "The Global Status of Carbon Capture and Storage 2023: Scaling Up Through 2030." Global Carbon Capture and Storage Institute. 98. https://res.cloudinary.com/dbtfcnfij/images/v1700717007/Global-Status-of-CCS-Report-Update-23-Nov/Global-Status-of-CCS-Report-Update-23-Nov.pdf?_i=AA.

Diaz-Chavez, R., G. Berndes, D. Neary, A. Elia Neto, and M. Fall. 2011. "Water Quality Assessment of Bioenergy Production." *Biofuels, Bioproducts and Biorefining* 5, no. 4: 445–463. https://doi.org/10.1002/bbb.319.

Dixon, A. P., D. Faber-Langendoen, C. Josse, J. Morrison, and C. J. Loucks. 2014. "Distribution Mapping of World Grassland Types." *Journal of Biogeography* 41, no. 11: 2003–2019. https://doi.org/10.1111/jbi.12381.

Donnison, C., R. A. Holland, A. Hastings, L. Armstrong, F. Eigenbrod, and G. Taylor. 2020. "Bioenergy With Carbon Capture and Storage (BECCS): Finding the Win–Wins for Energy, Negative Emissions and Ecosystem Services—Size Matters." *Global Change Biology. Bioenergy* 12, no. 8: 586–604. https://doi.org/10.1111/gcbb.12695.

Fajardy, M., and N. Mac Dowell. 2017. "Can BECCS Deliver Sustainable and Resource Efficient Negative Emissions?" *Energy & Environmental Science* 10, no. 6: 1389–1426. https://doi.org/10.1039/C7EE00465F.

Fajardy, M., J. Morris, A. Gurgel, H. Herzog, N. Mac Dowell, and S. Paltsev. 2021. "The Economics of Bioenergy With Carbon Capture and Storage (BECCS) Deployment in a 1.5°C or 2°C World." *Global Environmental Change* 68: 102262. https://doi.org/10.1016/j.gloenvcha.2021.102262.

FAO. 2020. "Global Forest Resources Assessment 2020." https://doi.org/10.4060/ca9825en.

FAO. 2024. "Land Statistics 2001–2022 – Global, Regional and Country Trends (FAOSTAT Analytical Briefs, No. 88)." https://doi.org/10.4060/cd1484en.

Felten, D., N. Fröba, J. Fries, and C. Emmerling, 2013. "Energy balances and greenhouse gas-mitigation potentials of bioenergy cropping systems (Miscanthus, rapeseed, and maize) based on farming conditions in Western Germany." *Renewable Energy* 55: 160–174.

Fridahl, M., and M. Lehtveer. 2018. "Bioenergy With Carbon Capture and Storage (BECCS): Global Potential, Investment Preferences, and Deployment Barriers." *Energy Research & Social Science* 42: 155–165. https://doi.org/10.1016/j.erss.2018.03.019.

García-Freites, S., C. Gough, and M. Röder. 2021. "The Greenhouse Gas Removal Potential of Bioenergy With Carbon Capture and Storage (BECCS) to Support the UK's Net-Zero Emission Target." *Biomass and Bioenergy* 151: 106164. https://doi.org/10.1016/j.biombioe.2021.106164.

Gelfand, I., S. K. Hamilton, A. N. Kravchenko, R. D. Jackson, K. D. Thelen, and G. P. Robertson. 2020. "Empirical Evidence for the Potential Climate Benefits of Decarbonizing Light Vehicle Transport in the U.S. With Bioenergy From Purpose-Grown Biomass With and Without BECCS." *Environmental Science & Technology* 54, no. 5: 2961–2974. https://doi.org/10.1021/acs.est.9b07019.

Gelfand, I., R. Sahajpal, X. Zhang, R. C. Izaurralde, K. L. Gross, and G. P. Robertson. 2013. "Sustainable Bioenergy Production From Marginal Lands in the US Midwest." *Nature* 493: 514–517. https://doi.org/10.1038/nature11811.

Gerstner, K., C. F. Dormann, A. Stein, A. M. Manceur, and R. Seppelt. 2014. "Effects of Land Use on Plant Diversity – A Global Meta-Analysis." *Journal of Applied Ecology* 51, no. 6: 1690–1700. https://doi.org/10.1111/1365-2664.12329.

Grass, I., J. Loos, S. Baensch, et al. 2019. "Land-Sharing/−Sparing Connectivity Landscapes for Ecosystem Services and Biodiversity Conservation." *People and Nature* 1, no. 2: 262–272. https://doi.org/10.1002/pan3.21.

Guo, M., W. Song, and J. Buhain. 2015. "Bioenergy and Biofuels: History, Status, and Perspective." *Renewable and Sustainable Energy Reviews* 42: 712–725. https://doi.org/10.1016/j.rser.2014.10.013.

Hanssen, S. V., V. Daioglou, Z. J. N. Steinmann, J. C. Doelman, D. P. Van Vuuren, and M. A. J. Huijbregts. 2020. "The Climate Change Mitigation Potential of Bioenergy With Carbon Capture and Storage." *Nature Climate Change* 10, no. 11: 1023–1029. https://doi.org/10.1038/s41558-020-0885-y.

Hanssen, S. V., Z. J. N. Steinmann, V. Daioglou, M. Čengić, D. P. Van Vuuren, and M. A. J. Huijbregts. 2022. "Global Implications of Crop-Based Bioenergy With Carbon Capture and Storage for Terrestrial Vertebrate Biodiversity." *Global Change Biology. Bioenergy* 14, no. 3: 307–321. https://doi.org/10.1111/gcbb.12911.

Harris, Z. M., G. Alberti, M. Viger, et al. 2017. "Land-Use Change to Bioenergy: Grassland to Short Rotation Coppice Willow Has an Improved Carbon Balance." *Global Change Biology. Bioenergy* 9, no. 2: 469–484. https://doi.org/10.1111/gcbb.12347.

Heck, V., D. Gerten, W. Lucht, and A. Popp. 2018. "Biomass-Based Negative Emissions Difficult to Reconcile With Planetary Boundaries." *Nature Climate Change* 8, no. 2: 151–155. https://doi.org/10.1038/s41558-017-0064-y.

Hersbach, H., B. Bell, P. Berrisford, et al. 2023. "ERA5 Hourly Data on Single Levels From 1940 to Present." Copernicus Climate Change Service Climate Data Store. https://doi.org/10.24381/cds.adbb2d47.

Immerzeel, D. J., P. A. Verweij, F. Van Der Hilst, and A. P. C. Faaij. 2014. "Biodiversity Impacts of Bioenergy Crop Production: A State-Of-The-Art Review." *Global Change Biology. Bioenergy* 6, no. 3: 183–209. https://doi.org/10.1111/gcbb.12067.

Klein, D., G. Luderer, E. Kriegler, et al. 2014. "The Value of Bioenergy in Low Stabilization Scenarios: An Assessment Using REMIND-MAgPIE." *Climatic Change* 123, no. 3–4: 705–718. https://doi.org/10.1007/s10584-013-0940-z.

Kravchenko, A. N., and G. P. Robertson. 2011. "Whole-Profile Soil Carbon Stocks: The Danger of Assuming Too Much From Analyses of Too Little." *Soil Science Society of America Journal* 75, no. 1: 235–240.

Lark, T. J., N. P. Hendricks, A. Smith, et al. 2022. "Environmental Outcomes of the US Renewable Fuel Standard." *Proceedings of the National Academy of Sciences* 119, no. 9: e2101084119. https://doi.org/10.1073/pnas.2101084119.

Le Noë, J., S. Manzoni, R. Abramoff, et al. 2023. "Soil Organic Carbon Models Need Independent Time-Series Validation for Reliable Prediction." *Communications Earth & Environment* 4, no. 1: 158. https://doi.org/10.1038/s43247-023-00830-5.

Lei, C., M. Abraha, J. Chen, and Y.-J. Su. 2021. "Long-Term Variability of Root Production in Bioenergy Crops From Ingrowth Core Measurements." *Journal of Plant Ecology* 14, no. 5: 757–770. https://doi.org/10.1093/jpe/rtab018.

Lei, C., J. Chen, and G. P. Robertson. 2023. "Climate Cooling Benefits of Cellulosic Bioenergy Crops From Elevated Albedo." *Global Change Biology. Bioenergy* 15, no. 11: 1373–1386. https://doi.org/10.1111/gcbb.13098.

Lu, D., D. Ricciuto, A. Walker, C. Safta, and W. Munger. 2017. "Bayesian Calibration of Terrestrial Ecosystem Models: A Study of Advanced Markov Chain Monte Carlo Methods." *Biogeosciences* 14, no. 18: 4295–4314.

Luehmann, M. D., B. G. Peter, C. B. Connallon, et al. 2016. "Loamy, Two-Storied Soils on the Outwash Plains of Southwestern Lower Michigan: Pedoturbation of Loess With the Underlying Sand." *Annals of the American Association of Geographers* 106, no. 3: 551–572. https://doi.org/10.1080/00045608.2015.1115388.

Ma, J., L. Li, H. Wang, et al. 2022. "Carbon Capture and Storage: History and the Road Ahead." *Engineering* 14: 33–43. https://doi.org/10.1016/j.eng.2021.11.024.

Mahabbati, A., J. Beringer, M. Leopold, et al. 2021. "A Comparison of Gap-Filling Algorithms for Eddy Covariance Fluxes and Their Drivers." *Geoscientific Instrumentation, Methods and Data Systems* 10, no. 1: 123–140. https://doi.org/10.5194/gi-10-123-2021.

McCalmont, J. P., N. P. McNamara, I. S. Donnison, K. Farrar, and J. C. Clifton-Brown. 2017. "An Interyear Comparison of CO_2 Flux and Carbon Budget at a Commercial-Scale Land-Use Transition From Semi-Improved Grassland to *Miscanthus* x *Giganteus*." *Global Change Biology. Bioenergy* 9, no. 1: 229–245. https://doi.org/10.1111/gcbb.12323.

McDaniel, M. D., D. Saha, M. G. Dumont, M. Hernández, and M. A. Adams. 2019. "The Effect of Land-Use Change on Soil CH_4 and N_2O Fluxes: A Global Meta-Analysis." *Ecosystems* 22, no. 6: 1424–1443. https://doi.org/10.1007/s10021-019-00347-z.

Melnikova, I., P. Ciais, K. Tanaka, N. Vuichard, and O. Boucher. 2023. "Relative Benefits of Allocating Land to Bioenergy Crops and Forests Vary by Region." *Communications Earth & Environment* 4, no. 1: 230.

Moffat, A. M., D. Papale, M. Reichstein, et al. 2007. "Comprehensive Comparison of Gap-Filling Techniques for Eddy Covariance Net Carbon Fluxes." *Agricultural and Forest Meteorology* 147, no. 3–4: 209–232. https://doi.org/10.1016/j.agrformet.2007.08.011.

Muri, H. 2018. "The Role of Large—Scale BECCS in the Pursuit of the 1.5°C Target: An Earth System Model Perspective." *Environmental Research Letters* 13, no. 4: 44010.

Neubauer, S. C., and J. P. Megonigal. 2015. "Moving Beyond Global Warming Potentials to Quantify the Climatic Role of Ecosystems." *Ecosystems* 18, no. 6: 1000–1013. https://doi.org/10.1007/s10021-015-9879-4.

Neubauer, S. C., and J. P. Megonigal. 2019. "Correction to: Moving Beyond Global Warming Potentials to Quantify the Climatic Role of Ecosystems." *Ecosystems* 22, no. 8: 1931–1932. https://doi.org/10.1007/s10021-019-00422-5.

Paciorek, C. J., C. V. Cogbill, J. A. Peters, et al. 2021. "The Forests of the Midwestern United States at Euro-American Settlement: Spatial and Physical Structure Based on Contemporaneous Survey Data." *PLoS One* 16, no. 2: e0246473. https://doi.org/10.1371/journal.pone.0246473.

Pett-Ridge, J., S. Kuebbing, A. Mayer, et al. 2023. "Roads to Removal: Options for Carbon Dioxide Removal in the United States." https://doi.org/10.2172/2301853.

Quader, M. A., and S. Ahmed. 2017. "Bioenergy With Carbon Capture and Storage (BECCS): Future Prospects of Carbon-Negative Technologies." In *Clean Energy For Sustainable Development*, 91–140. UK: Elsevier. https://doi.org/10.1016/B978-0-12-805423-9.00004-1.

Ramírez, P. B., S. Mosier, F. Calderón, and M. F. Cotrufo. 2022. "Using Mid-Infrared Spectroscopy to Optimize Throughput and Costs of Soil Organic Carbon and Nitrogen Estimates: An Assessment in Grassland Soils." *Environments* 9, no. 12: 149.

Reichstein, M., E. Falge, D. Baldocchi, et al. 2005. "On the Separation of Net Ecosystem Exchange Into Assimilation and Ecosystem Respiration: Review and Improved Algorithm." *Global Change Biology* 11, no. 9: 1424–1439. https://doi.org/10.1111/j.1365-2486.2005.001002.x.

Robertson, G. P., S. K. Hamilton, B. L. Barham, et al. 2017. "Cellulosic Biofuel Contributions to a Sustainable Energy Future: Choices and Outcomes." *Science* 356, no. 6345: eaal2324. https://doi.org/10.1126/science.aal2324.

Roe, S., C. Streck, M. Obersteiner, et al. 2019. "Contribution of the Land Sector to a 1.5°C World." *Nature Climate Change* 9, no. 11: 817–828. https://doi.org/10.1038/s41558-019-0591-9.

Rosa, L., D. L. Sanchez, and M. Mazzotti. 2021. "Assessment of Carbon Dioxide Removal Potential Via BECCS in a Carbon-Neutral Europe." *Energy & Environmental Science* 14, no. 5: 3086–3097. https://doi.org/10.1039/D1EE00642H.

Shepherd, A., M. Martin, and A. Hastings. 2021. "Uncertainty of Modelled Bioenergy With Carbon Capture and Storage Due to Variability of Input Data." *Global Change Biology. Bioenergy* 13, no. 4: 691–707. https://doi.org/10.1111/gcbb.12803.

Shuai, Y., J. G. Masek, F. Gao, and C. B. Schaaf. 2011. "An Algorithm for the Retrieval of 30-m Snow-Free Albedo From Landsat Surface Reflectance and MODIS BRDF." *Remote Sensing of Environment* 115, no. 9: 2204–2216. https://doi.org/10.1016/j.rse.2011.04.019.

Shuai, Y., J. G. Masek, F. Gao, C. B. Schaaf, and T. He. 2014. "An Approach for the Long-Term 30-m Land Surface Snow-Free Albedo Retrieval From Historic Landsat Surface Reflectance and MODIS-Based a Priori Anisotropy Knowledge." *Remote Sensing of Environment* 152: 467–479. https://doi.org/10.1016/j.rse.2014.07.009.

Smith, P., J. Adams, D. J. Beerling, et al. 2019. "Land-Management Options for Greenhouse Gas Removal and Their Impacts on Ecosystem Services and the Sustainable Development Goals." *Annual Review of Environment and Resources* 44, no. 1: 255–286. https://doi.org/10.1146/annurev-environ-101718-033129.

Smith, P., J. Soussana, D. Angers, et al. 2020. "How to Measure, Report and Verify Soil Carbon Change to Realize the Potential of Soil Carbon Sequestration for Atmospheric Greenhouse Gas Removal." *Global Change Biology* 26, no. 1: 219–241. https://doi.org/10.1111/gcb.14815.

Stoy, P. C., S. Ahmed, M. Jarchow, et al. 2018. "Opportunities and Trade-Offs Among BECCS and the Food, Water, Energy, Biodiversity, and Social Systems Nexus at Regional Scales." *Bioscience* 68, no. 2: 100–111. https://doi.org/10.1093/biosci/bix145.

Thornton, M. M., R. Shrestha, Y. Wei, P. E. Thornton, S.-C. Kao, and B. E. Wilson. 2022. "Daymet: Daily Surface Weather Data on a 1-km Grid for North America, Version 4 R1." ORNL DAAC, Oak Ridge, Tennessee, USA. https://doi.org/10.3334/ORNLDAAC/2129.

Vogel, E., D. Deumlich, and M. Kaupenjohann. 2016. "Bioenergy Maize and Soil Erosion—Risk Assessment and Erosion Control Concepts." *Geoderma* 261: 80–92. https://doi.org/10.1016/j.geoderma.2015.06.020.

Wang, Z., C. B. Schaaf, Q. Sun, et al. 2017. "Monitoring Land Surface Albedo and Vegetation Dynamics Using High Spatial and Temporal Resolution Synthetic Time Series From Landsat and the MODIS BRDF/NBAR/Albedo Product." *International Journal of Applied Earth Observation and Geoinformation* 59: 104–117. https://doi.org/10.1016/j.jag.2017.03.008.

Ward, N. D., T. S. Bianchi, P. M. Medeiros, et al. 2017. "Where Carbon Goes When Water Flows: Carbon Cycling Across the Aquatic Continuum." *Frontiers in Marine Science* 4: 7. https://doi.org/10.3389/fmars.2017.00007.

Werling, B. P., T. L. Dickson, R. Isaacs, et al. 2014. "Perennial Grasslands Enhance Biodiversity and Multiple Ecosystem Services in Bioenergy Landscapes." *Proceedings of the National Academy of Sciences* 111, no. 4: 1652–1657. https://doi.org/10.1073/pnas.1309492111.

Wood, S. N. 2017. *Generalized Additive Models: An Introduction With R*. New York: Chapman and Hall/CRC.

Wutzler, T., A. Lucas-Moffat, M. Migliavacca, et al. 2018. "Basic and Extensible Post-Processing of Eddy Covariance Flux Data With REddyProc." *Biogeosciences* 15, no. 16: 5015–5030. https://doi.org/10.5194/bg-15-5015-2018.

Zhang, Y., J. M. Lavallee, A. D. Robertson, et al. 2021. "Simulating Measurable Ecosystem Carbon and Nitrogen Dynamics With the Mechanistically Defined MEMS 2.0 Model." *Biogeosciences* 18, no. 10: 3147–3171. https://doi.org/10.5194/bg-18-3147-2021.

Supporting Information

Additional supporting information can be found online in the Supporting Information section.